

# Chapter 13

## Temperature Dependent Micromechanical Testing on the Formation of Cu/Sn Intermetallic Thin Films

F.-C. Hsu, F.-C. Lu, C.-T. Huang, and M.-T. Lin

**Abstract** A temperature controlled tensile testing was performed to investigate the influence of external stress on the growth of an interfacial Cu-Sn IMC layer. The test specimens were prepared by depositing 25  $\mu\text{m}$  layers of tin atop of copper substrate using electroplating. Samples were then clamped in a micromechanical testing apparatus integrated with a furnace. Experiments were carried out using load feedback control to provide constant load on the specimens with the stress level of 50, 100 and 150 MPa under constant temperature at 200 °C for 3–5 h annealing. Comparisons were made between samples undergoing stresses and those without stresses annealing. We observed the influence of stress levels and aging time on the formation of intermetallic compounds (IMC). Stress does influence the formation of Cu/Sn IMC. The thickness of IMC increased under stress. The growth rate of IMC was faster in stressed tin samples. Moreover, the formation of IMC micrographic structures under external stress differs considerably according to the level of stress.

**Keywords** Stress effect • Cu-Sn IMC • Tensile testing • Interdiffusion • High temperature tensile testing

### 13.1 Introduction

The fabrication of a dependable solder plays an important role in microelectronic packages due to its role on the interconnect joint of the microelectronic device packages. In practical, a microelectronics joint was generated from the formation of an inter-metallic compound at the interface between the solder and substrate materials such as Pb, Cu, Ag or Ni. Currently, the industry is facing an environmental demand for increased use of Pb-free solders [1]. Many of the leading solder alloy candidates for Pb-Sn solder replacement are based on the Sn-Cu system [2–4]. The primary concerns are the solderability and manufacturability using these Pb-free alloys. An understanding of reliability issues such as the microstructural evolution of a joint with time, temperature and stresses in as-prepared and aged joints has become an important need and the mechanical behaviors of Sn-based inter-metallics plays a significant role in determining the reliability of Pb-free solders [11–13].

In order to understand the stress effects on the solder reaction with Cu, especially during solid state aging, it is imperative to develop in-situ studies on the inter-metallic formation under stress. This study investigates the stress effect on the Sn-Cu interfacial reaction. Pure Cu plate was used as a sample substrate. Electroplated Sn film was deposited onto a Cu substrate as the sample [14, 15]. The sample was cut into a standard tensile specimen and placed inside a temperature controlled micro-tensile machine to exert tensile stress on the Sn-Cu films. The Sn-Cu interfacial reaction without the influence of stress was also studied as a reference for comparison.

---

F.-C. Hsu • F.-C. Lu • C.-T. Huang • M.-T. Lin (✉)

Graduate Institute of Precision Engineering, National Chung Hsing University, 250, Kuo-Kuang Rd., Taichung 40227, Taiwan, R.O.C.

e-mail: [mingtlin@nchu.edu.tw](mailto:mingtlin@nchu.edu.tw)

## 13.2 Experimental Detail

The sample was fabricated on a conventional 99.99 microelectronics grade copper sheet with a thickness of 400  $\mu\text{m}$ . After standard cleaning procedures, the samples exhibited uniformity prior to the experiments. Standard electroplating was used to deposit tin film on the copper substrate to a thickness of 25  $\mu\text{m}$ . The samples were then cut into strips 90 mm in length and 5 mm in width.

The Hung Ta Instrument Co. HT-2402 tensile testing system was used with extensive modifications to make it suitable for elevated-temperature testing in the present study. The features of the testing system are detail in Figs. 13.1 and 13.2. As the primary goal was to investigate stress effect in intermetallic formation at elevated temperature, a major experimental concern was to limit thermal drift – and the associated thermally induced strains – in the system. To this end, the apparatus

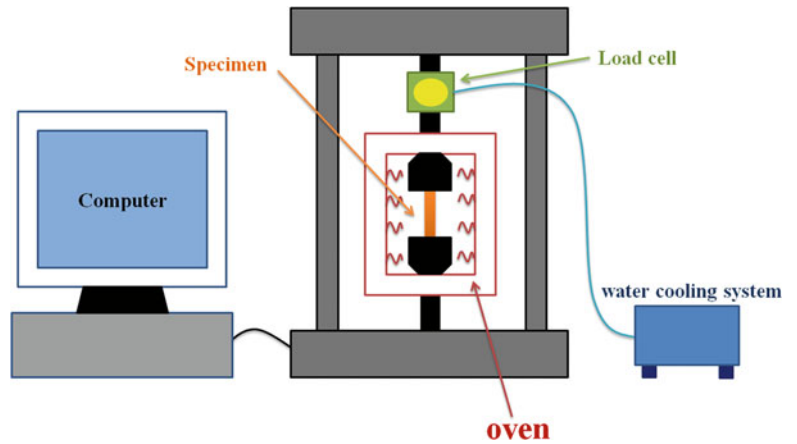


**Fig. 13.1** Schematic view of the system



**Fig. 13.2** Schematic image of the system

**Fig. 13.3** Schematic of loading on a sample, it shows the feedback control of load if stress relaxation of the sample occurs during the experiment

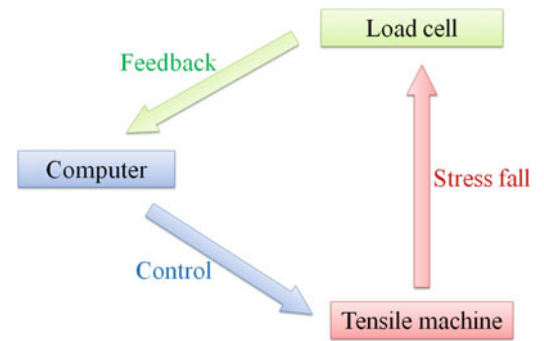


**Table 13.1** The parameters used to calculate stress values in the experiments

$\sigma$ (MPa)	A(mm <sup>2</sup> )	F(N)	Kgw
50	2.125	106.25	10.84
100	2.125	212.5	21.68
150	2.125	318.75	32.53

was mounted inside a temperature-controlled enclosure. This, and other features of the test system, made it possible to conduct elevated-temperature tests up to 200 °C with durations on the order of several days.

In preparation for mechanical testing, the samples were clamped into ceramic grips. The loading clamp was sufficiently aligned to accommodate four specimens simultaneously. Two unloaded control specimens were placed in close proximity to the loaded specimens in each run to account for variations in the experimental conditions from run to run. A typical test history involved constant strain rate straining to a predetermined stress level, a constant stress period duration with load feedback to eliminate stress relaxation effect, then constant strain unloading followed by a zero load hold period. Strain rates for the loading/unloading phases were 10 kgf/min.

In order to avoid creep or stress relaxation on the specimen, one program was executed to give tensile on the specimen by the actuator with constant load amplitude. At the same time, another program was performed to calculate the apparent stresses acquired from the data acquisition signals recorded from load cell to compare with the controlled stress signals and decided if it is necessary to adjust the actuator to maintain constant stress loading at all time (Fig. 13.3).

Test results were obtained for the same amounts of tensile stress with respect to the control. To apply greater stress effect on the Cu/Sn interface, we designed the experiment to provide stress values of 50, 100 and 150 MPa. Table 13.1 lists the parameters used to calculate stress values in the experiments.

After the samples were clamped, the furnace set to 200 °C was used to carry out the stressed aging procedure. Some samples were held without stress for as-soldered state testing. For the inter-metallic growth in this step, diffusion couples were annealed for times such that a copper-tin inter-metallic specimen could be formed. The annealing times were based on literature values for growth rates in diffusion couples [5, 6]. The diffusion process postulated in the literature [7] indicated that there are two major IMCs formed in Copper Tin annealing. Cu<sub>6</sub>Sn<sub>5</sub> is formed through short time annealing and Cu<sub>3</sub>Sn is formed through long time annealing.

Following aging, the samples were removed from the tensile testing system and mounted in epoxy resin for metallographical examination. The samples were ground and polished to expose cross-sections of the Sn/Cu interface. A high magnitude optical microscope was used to observe the formation of IMC at the Sn/Cu interface. Image processing was used to facilitate the measurement of areas in the cross-sections of the IMC resulting from the unevenness of the IMC layer along the interface and the linear length of the Cu/Sn interface. The thickness of IMC was determined by dividing the area by the linear length, as described in the literature [8, 9]. The reported thickness of the IMC is the average value of at least six measurements.

### 13.3 Results

Figure 13.4 shows optical micrographs of cross-sections of the Cu/Sn interface of sample after thermal aging at 200 °C for 72, 120 and 168 h with sample without stress, sample subjected to a 100 MPa tensile, sample subjected to a 150 MPa tensile stress. According to the elemental analysis results, two distinct phases were observed in all of the samples: the phase adjacent to the Cu side was identified as Cu<sub>3</sub>Sn; the phase next to the Sn side was Cu<sub>6</sub>Sn<sub>5</sub>. This indicates that the applied

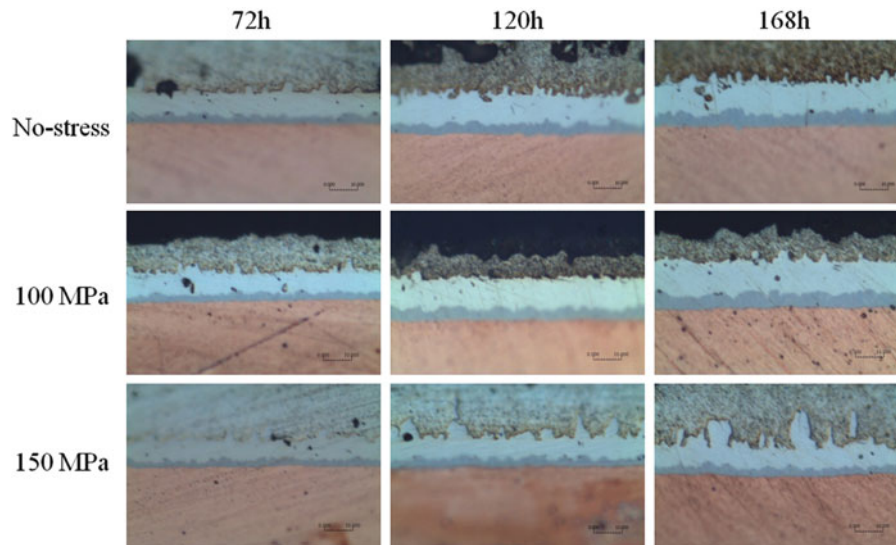


**Fig. 13.4** Micrographs showing cross-sections of the Sn/Cu interface of sample after thermal aging at 200 °C for 72, 120 and 168 h with sample without stress, sample subjected to a 100 MPa tensile, sample subjected to a 150 MPa tensile stress

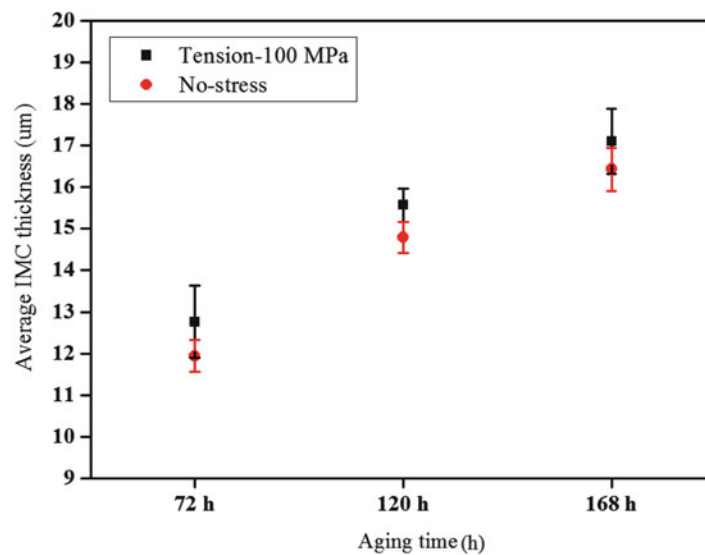


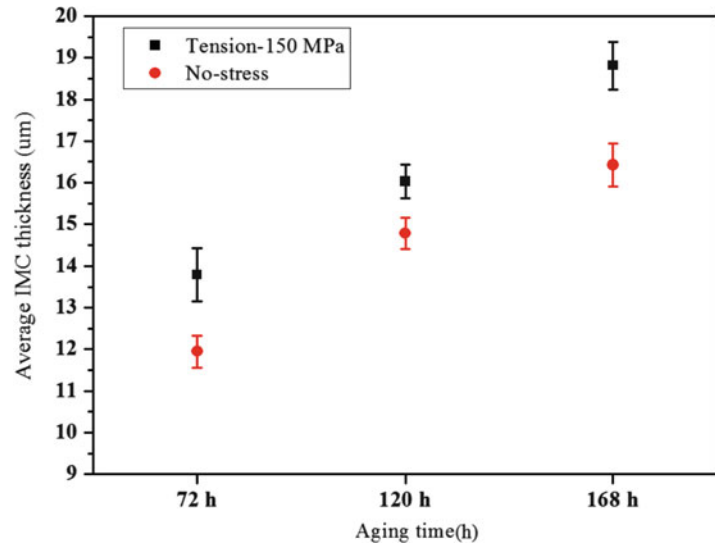
**Fig. 13.5** Total thickness of Sn/Cu IMC sample versus aging times for stress of 100 MPa tensile and unloaded control

external stress, regardless of whether the stress state, had no influence on either type of IMC. However, the growth rates of IMC ( $\text{Cu}_3\text{Sn} + \text{Cu}_6\text{Sn}_5$ ) were influenced by the applied stress. The thickness of the IMC film ( $\text{Cu}_3\text{Sn} + \text{Cu}_6\text{Sn}_5$ ) differed among each of the cases. For example, the results of total thickness of IMC after thermal aging at 200 °C for 72 h under 100 MPa tension (12.77  $\mu\text{m}$ ) was thicker than in the sample with no stress (11.95  $\mu\text{m}$ ). The no stress samples in Fig. 13.4 show common scallops in the structure of the IMC while the sample under high stress (150 MPa) reveals considerable distortion. The samples submitted to high stress contain a large number of islands of needle-like columnar Cu/Sn IMC enclosed by continuous large planar Cu/Sn IMC.

Figure 13.5 shows the total thickness of the Sn/Cu IMC as a function of aging time at 200 °C under film stress of 100 MPa and unloaded. Table 13.2 summarizes the thickness of Sn/Cu IMC under all test conditions. The growth rate of the Sn/Cu IMC exhibited characteristics that under tension grew at a rate higher than that with no stress. Figure 13.6 shows the total thickness of Sn/Cu IMC as a function of aging time at 200 °C under film stress of 150 MPa and unloaded. The growth rate of the Sn/Cu exhibited characteristics similar to those observed in Fig. 13.5, in which the Sn/Cu IMC under tension grew more rapidly than in samples without stress. This indicates that tensile stress enhances the growth of the Sn/Cu IMC. In addition,

**Table 13.2** Sn/Cu IMC thickness as a function of annealing time under tensile stress conditions (unit:  $\mu\text{m}$ )

Stress(MPa) \ Time(h)	72h	120h	168h
No-stress	11.945 $\pm$ 0.383	14.782 $\pm$ 0.378	16.425 $\pm$ 0.517
100 MPa	12.766 $\pm$ 0.86	15.559 $\pm$ 0.407	17.102 $\pm$ 0.779
150 MPa	13.787 $\pm$ 0.631	16.033 $\pm$ 0.407	18.816 $\pm$ 0.577

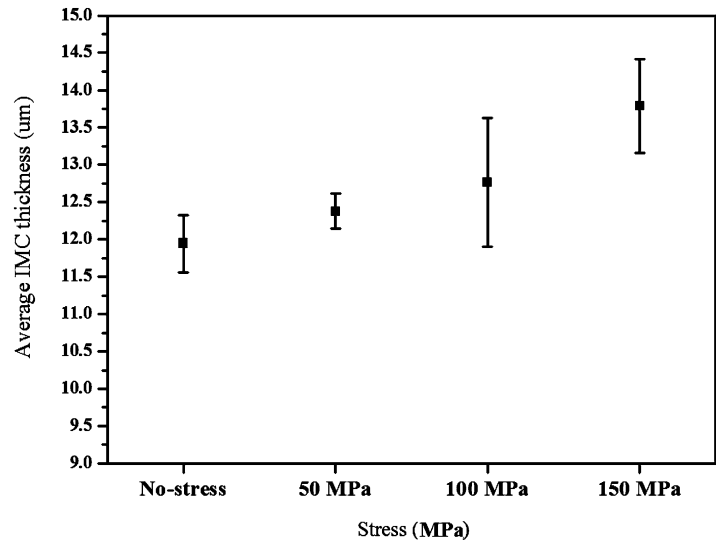
**Fig. 13.6** Total thickness of Sn/Cu IMC sample versus aging times for stress of 150 MPa tensile and unloaded control

the overall IMC growth rates under higher stress samples exceed those of lower stress samples. Figure 13.7 illustrates the thickness of IMC samples as a function of film stress after thermal aging at 200 °C for 72 h. The error bars shown for each point indicate the minimum and maximum observed increase. The data points indicate mean values.

In almost every sample, tensile stress influenced the growth of Sn/Cu IMC. Interestingly, the enhancement of growth in IMCs is strongly related with the increase of tensile stress. In the following, we discuss the diffusion behavior of components in the Sn/Cu interfacial reaction to gain a deeper understanding of the influence of external stress on IMC growth. During the isothermal aging of Cu and Sn films, Cu diffuses interstitially into Sn, leading to the assumption that Cu diffusion into Sn is the dominant process. Therefore, Cu is thought to be the faster diffusing species in Sn/Cu interfacial reactions [7, 10], and the growth of the Cu-Sn IMCs depends primarily upon Cu diffusion into Sn. Two major driving forces are involved in the diffusion behavior in the Sn/Cu interfacial reaction in the tested samples: (1) the typical concentration gradient and (2) the stress gradient. For samples without stress, the diffusion of Cu into Sn is driven only by the concentration gradient.

Because the participation of even higher stress in tin samples can create voids or defects in the solder matrix, it is not surprising to observe more distorted needle-like columnar islands in the samples under stress. The large number of distorted columnar islands in the samples under 150 MPa (Fig. 13.4) reveals that increased stress could be the driving force behind the outward diffusion of Cu into the solder. We observed this micrographic structure in the interfacial reaction of Sn/Cu samples subjected to a higher tensile stress. This leads us to believe that could create an inhomogeneous local strain field through the formation of voids or defects in the solder matrix. This phenomenon could be amplified through the application of external stress. As a result, we observed distorted needle-like columnar islands in the Cu/Sn IMC. Thus the diffusivity of Cu was increased since Cu diffusion in the tin lattice under tension was facilitated. As a result, the growth rate of IMC was also enhanced.

**Fig. 13.7** Total thickness of Sn/Cu IMC sample versus stress of 50, 100 and 150 MPa after thermal aging at 200 °C for 72 h



### 13.4 Conclusions

In this paper, we reported on a temperature controlled micro-tensile measurement results of the stress effect related to interfacial Cu-Sn IMC layer growth. The proposed method allows interfacial Cu-Sn IMC layer growth observation under tension. The results indicated that tensile stress would affect Cu-Sn inter-metallic formation. We observed the influence of stress levels and aging time on the formation of intermetallic compounds (IMC). Stress does influence the formation of Cu/Sn IMC. The thickness of IMC increased under stress. The growth rate of IMC was faster in stressed tin samples. Moreover, the formation of IMC micrographic structures under external stress differs considerably according to the level of stress. The enhanced effect caused by the larger stress was somewhat more severe than that due to smaller tensile stress. We hypothesize that the observed IMC thickness increase is related to stress enhanced out-diffusion of Cu towards the solder and strain in the lattice at the diffusion interface.

### References

1. Tu KN (1973) Interdiffusion and reaction in bimetallic Cu-Sn thin films. *Acta Metall* 21:347–354
2. Rymaszewski EJ, Tummala RR, Watari T (1997) *Microelectronic packaging handbook*, Part I, 2nd edn. Chapman and Hall, Springer US
3. Harper CA (2005) *Electronic packaging and interconnection handbook*. McGraw-Hill, New York
4. Zarrow P (1999) On the forefront: lead free: don't fight a fact, deal with it! *Circ Assem* 10:18–20
5. [http://www.tycoelectronics.com/customersupport/rohssupportcenter/pdf/2010\\_CALCE\\_Tin\\_Whsker\\_Conference\\_TE.pdf](http://www.tycoelectronics.com/customersupport/rohssupportcenter/pdf/2010_CALCE_Tin_Whsker_Conference_TE.pdf)
6. Snog JY, Jin Yu, Lee TY (2004) Effects of reactive diffusion on stress evolution in Cu–Sn films. *Scripta Materialia* 51:167–170
7. Ngoh SL, Zhou W, Pang HL, Spowage AC, Shi XQ (2004) Effect of stress on interfacial intermetallic compound development of Sn-Ag-Cu Lead-free solder joint on Au/Ni/Cu substrate. *Electronics packaging technology conference*, Singapore
8. King-Ning Tu (2007) *Solder joint technology*. Springer, New York
9. [http://www.tycoelectronics.com/customersupport/rohssupportcenter/pdf/tyco\\_electronics\\_hilty\\_ipc\\_Boston\\_2005.pdf](http://www.tycoelectronics.com/customersupport/rohssupportcenter/pdf/tyco_electronics_hilty_ipc_Boston_2005.pdf)
10. Huh JY, Moon SJ (2000) Effect of elastic stresses on solid-state amorphization of Zr/Co multilayers. *Thin Solid Films* 377–378:611–616
11. Mulugeta Abteu, Selvaduray G (2000) Lead-free solder in microelectronics. *Mater Sci Eng* 27:95–141
12. Daniel L, Wong CP (2009) *Material for advanced packaging*. Springer, New York
13. Görlich J, Schmitz G, Tu KN (2005) On the mechanism of the binary Cu/Sn solder reaction. *J Appl Phys Lett* 86:053106-1–053106-3
14. Kakeshita T, Shimizu K, Kawanaka R et al (1982) Grain size effect of electro-plated tin coatings on whisker growth. *J Mater Sci* 17:2560–2566
15. Lee Z, Lee DN (1998) Spontaneous growth mechanism of tin whisker. *Acta Metal* 46:3701–3714